Egypt. J. Chem. **Vol. 65**, No. 9 pp. 497 - 511 (2022)

Egyptian Journal of Chemistry

http://ejchem.journals.ekb.eg/

Zinc oxide nanoparticles characterization and therapeutic evaluation on high fat / sucrose diet induced-obesity

Ahmed M. A. El-Seidy,[1] Samir A Bashandy,[2] Fatma A. A. Ibrahim, [3] Sahar S. Abd El-Rahman,[4] Omar Farid, [5] Sherif Moussa, [3] Marwan A. El-Baset[2]

[1] Inorganic Chemistry Department National Research Centre, 33 El-Bohouth St., P.O. 12622, Dokki, Cairo, Egypt.

[2] Pharmacology Department, Medical Research and Clinical Studies Institute, National Research Centre, 33 El-Bohouth St., Dokki, P.O. 12622, Cairo, Egypt, [3] Biochemistry Dept, Biotechnology Institute, National Research Centre, 33 EL BohouthSt., Dokki, Cairo, Egypt, [4] Pathology Dept, Faculty of Veterinary Medicine, Cairo University, [5] Researcher, National organization of drug control and research

Abstract

ZnO/KCl nanocomposite was prepared by solgel to appreciate the role of synthesized ZnO-NPs to curb obesity in a high-fat diet rat model. KCl played an important role in decreasing the particle size (30 nm) and also in facilitating the suspension formation of ZnO-NPs. XRD and HRTEM were carried out to estimate the particle size while SEM was used to investigate the morphology of the nanoparticles. XPS measurements were used to examine the chemical compositions of the nanocomposite. XRD declared that ZnO has a hexagonal wurtzite structure. The Rietveld refinement has also been executed (chi^2 = 1.0 and R-factor was 0.05). The treatment of obese rats with ZnO-NPs enhanced the adiponectin level, hepatic carnitine (Car) and reduced hepatic glutathione (GSH) with lowering the liver enzymes and pathological changes. The treatment coused a decrease in body weight gain, Body mass index (BMI), leptin level, cholesterol, triglycerides, glucose, immunohistochemistry for nuclear factor kappa (NFκB), the insulin resistance index (HOMA-IR) and a reduction in hepatic malondialdehyde (MDA), nitric oxide (NO), and 8-Hydroxy-2'-deoxyguanosine (8OHdG). The results indicated a positive correlation between BMI and oxidative stress parameters. In conclusion, ZnO-NPs manifested valuable anti-obesity effects via lowering body weight gain, oxidative stress, BMI, lipids, and insulin resistance.

Keywords: ZnO-Nps, Rietveld analysis, obesity, metabolic syndrome, inflammatory markers, oxidative stress.

1- Introduction

Nanomaterials have unparalleled chemical and physical properties, enormous surface area to mass proportion and high reactivity. These properties can be used to solve some of the obstacles in the therapeutic and diagnostic representatives [1]. In a nanoscale, ZnO is one of the most valuable metal oxides; it is characterized by distinctive chemical and physical properties and participates in diverse biomedical fields such as biomedical imaging, drug delivery, gene delivery, and biosensing of a wide array of molecules [2]. Medically, ZnO-NPs exhibited antibacterial, antidiabetic, antioxidant and anticancer effects [3,4]. Zinc is a primary trace mineral element and has an important function in the metabolism of lipids in the liver. It stimulates lipophagy in hepatic cells, decreasing lipid accumulation and promoting lipolysis [5]. ZnO-NPs conquer liver fibrosis induced experimentally by thioacetamide and modulate liver enzymes via reducing oxidative stress [6]. ZnO-NPs lowered hepatic steatosis and peripheral insulin resistance result from non-alcoholic fatty liver disease [7]. ZnO-NPs showed anti-inflammatory properties as they downregulate the level of iNOS, COX-2, IL-1b, IL-6 and TNF-α [8]. In young obese women, there is a negative association between zinc consumption and IL-6 or leptin levels, indicating that zinc may have a substantial impact on obesity-related inflammation [9]. Supplementing obese people with zinc reduced their BMI, body weight, and triglyceride levels while having no effect on their lipid profile or glucose level. Obese persons may benefit from zinc as a complementary treatment [10]. Zn is required for the activity of enzymes associated with energy metabolism. It also affects the hormones which regulate body fat, including leptin, insulin, and adiponectin [11].

It is well known that bad lifestyle behaviors, such as unhealthy dietary habits are associated with many negative health consequences like weight gain and

*Corresponding author e-mail: ahmedmaee2@gmail.com (Ahmed M. A. El-Seidy)
Received date 23 December 2021; revised date 10 January 2022; accepted date 19 January 2022
DOI: 10.21608/EJCHEM.2022.112166.5113

obesity. The Western diet is heavy in carbohydrates including fructose and sucrose, and saturated fat (high caloric diet), leading to metabolic syndrome and non-alcoholic fatty liver problems [12]. Obesity develops when there is an energy imbalance among calories consumed and calories expended. A body mass index is implicated in the description of obesity [13]. Obesity, a nutritional disorder, has become predominant in many countries worldwide. Overweight people's account for around 2 billion people, with one-third of them being obese [14]. Obesity has been accompanied with some health complications as non-alcoholic fatty liver disease (NAFLD), type 2 diabetes mellitus, metabolic syndrome, hyperlipidemia, cardiovascular disease, and hypertension [15]. NAFLD was shown to have significant amounts of fat accumulation (steatosis), inflammation, cell death, and fibrosis in the liver [16,17]. High ALT levels, triglycerides, glucose, insulin, and blood pressure were found in Egyptian obese adolescents with NAFLD, although low HDL-C levels were found [18]. The link between obesity and inflammation has been well concluded from an elevation in the levels of cytokines recognized in obese patient[19]. Obesity is associated with high levels of free fatty acids, which increase the formation of oxygen free radicals, resulting in oxidative stress and insulin sensitivity [20]. Adipokines have a role in the progression of obesity-related insulin resistance [21]. The purpose of our study is the evaluation of efficacy of ZnO-NPs in the treatment of obesity and its complications via the study of inflammatory markers, oxidative stress, lipid profile and dipocyte hormones.

2- Experimental

2.1- Synthesis of ZnO/KCl nanocomposite

The nanocomposite was synthesized using sol–gel method. Practically, 2 g of polyethylene glycol (8000 LR) was dissolved in 480 mL of DD (double distilled water). The resulting solution was divided into two equal portions to dissolve 6.28 g of zinc chloride ($ZnCl_2$, 46.07 mmol) and 10.11 g of zinc acetate dihydrate ($Zn(CH_3COO)_2.2H_2O$, 46.07 mmol), respectively. The solution of the latter was added slowly (over 30 m) with constant stirring (1000 rpm) at 80° C to the former then potassium hydroxide solution (2.58 g KOH, 46.07 mmol in 100 mL DD) was added drop-wisely (over 50 m). After converting the solution into a gel, it was dried before being crushed into granules, calcined at 600°C for four hours in an air environment in a furnace and then crushed again.

2.2- Experimental systems

The XRD patterns were obtained from X'pert PRO diffractometer with a Cu-radiation (λ = 1.542Å) at 45 K.V. and 35mA over the range of 2θ =2° - 60° and the average size of the crystallites was calculated by Debye-Scherrer equation. Morphology was examined under SEM Philips apparatus, USA, type QUANTA FEG 250. The morphology, surface structure and size of the powder were examined under a transmission electron microscope. HR-TEM was carried out using TEM model JEOL 2100 LB6 transmission electron microscope at the National Research Center, Cairo, Egypt. XPS was collected on K-ALPHA (Thermo Fisher Scientific, USA) with monochromatic X-ray Al K-alpha radiation -10 to 1350 e.v spot size 400 micro m at pressure 10^{-9} mbar with full spectrum pass energy 200 e.v and at narrow spectrum 50 e.v.

2.3- Experimental Protocol

Thirty-two Wistar adult male rats at the age of 10 weeks weighing 138-155 g (Animal house of National Research Center, Egypt) were stayed at stable room temperature (25 C°) with a 12 h light/dark cycle and free access to food and water. The animals were left a week for adaptation. Eight rats were kept as control and others were given a high-fat diet and water from the tap with 25% sucrose for 16 weeks to develop obesity. The high-fat diet consists of carbohydrate 42.3%, protein 17%, fat 22.50%, fiber 3,2%, minerals 5%, and moisture 10%. Normal rats were fed free standard chow pellets.

The rats were separated into 4 groups: -

1st Group: Normal rats served as control

2nd Group: Obese rats injected with the same volume of vehicle

3rd Group: Obese rats treated with 5mg/Kg ZnO-NPs (IP injection) for 6 weeks

4th Group: Obese rats treated with 10mg/Kg ZnO-NPs (IP injection) for 6 weeks

The doses of ZnO-NPs used were according to previous work [6]. ZnO-NPs were suspended in distilled water. Animal handling was carried out according to recommendations and under Animal Care and Use of National Research Centre regulations in Egypt with ethical approval No.19218. All surgery was performed under anesthesia, and efforts were made to reduce suffering.

2.4- Anthropometric measures

Body mass index (BMI) can be calculated depending on the height and weight of the rat according to the formula: "BMI = body weight (g)/height (cm)". The circumference of the waist was measured. BMI was recorded at basal till the sixth week (two-week interval).

2.5- Samples

At the completion of the therapy period, the rats of all groups were fasted for about 10 hours. Blood samples were collected from a retro-orbital vein and separated plasma was stored in Eppendorf tubes at -30° for biochemical analysis.

Immediately after blood sampling, animals were sacrificed by cervical dislocation under ether anesthesia then livers were collected. A weighed part of the liver was homogenized with ice-cooled saline (0.9% NaCl) to prepare homogenate. The latter was then centrifuged at 3000 rpm for 10 min. at 5°C using a cooling centrifuge "Laborzentrifugen, Sigma, Germany". The supernatant was used for various analyses. The remaining portion of liver was fixed immediately in 10% neutral buffered formalin, processed for light microscopy to get (5µm) paraffin sections and stained with "Hematoxylin & Eosin (H &E)" to verify histological details. Furthermore, immunochemistry was performed on certain liver sections.

2.6- The adipocyte hormones

An immunoassay method was used to determine the levels of plasma leptin and adiponectin (ELISA, Sunlong Biotech Co. Kit, China).

2.7- Insulin resistance parameters

Blood glucose was determined calorimetrically following the instruction of the Salucea Company kit. Plasma insulin was assayed by immunoassay (ELISA) according to the instruction of Sunlong Biotech Co. Kit (China). Insulin resistance index (HOMA-IR) was estimated from the equation "(HOMA-IR): {(fasting glucose [mg/dL]) · (fasting insulin [µU/mL])} ÷ 405".

2.8- Liver function tests and lipid profile

AST, ALT, GGT, cholesterol, triglycerides, LDL, and HDL were calorimetrically determined in blood plasma using kits from the Salucea Company in the Netherlands.

2.9- Inflammatory markers

TNF-α, CRP, IL2, and IL6 levels were determined by the ELISA technique (Sunlong Biotech Co. Kit, China).

2.10- Hepatic Oxidative stress parameters

The levels of hepatic MDA, GSH, GSSG, NO, and Car were measured using an "Agilent HP 1200 series (USA) HPLC system" that included a quaternary pump, a column oven, Rheodine injector, and a 20 µl loop, as well as a UV variable wavelength detector. The sample concentration was determined from the resulting chromatogram using "Sigma Aldrich standard".

2.11- Determination of Hepatic ATP and 8-OHdG and AMP

The detection of ATP was done by HPLC [22]. Isolation and hydrolysis of hepatic DNA were performed as previously described [23]. The hydrolyzed mixture was centrifuged and the supernatant was injected into the HPLC. The separation of 8-OHDG was performed with an LC/Agilent 1200 series HPLC apparatus (USA) using UV detectors.

2.12- Histopathological and immunohistochemical evaluations

Formalin-fixed liver specimens of all groups were routinely processed for getting paraffin blocks, then serial sections of 4–5 µm were obtained and stained with hematoxylin and eosin (H&E). The histological lesions were described according to the criteria established by Brunt et al.[24], based on the percentage of involved hepatocytes and its zonal distribution, where; macro-vesicular steatosis is quantified (0 = absent; 1 (mild) < one third; 2 (moderate) = one to two-thirds; 3 (severe) > two-third), and the presence of micro-vesicular steatosis were recorded. Hepatocellular ballooning was evaluated for its zonal distribution as well as its severity (mild, marked) based on the numbers of hepatocytes showing this abnormality.

"Avidin-biotin peroxidase" technique "(DAB, Sigma Chemical Co.)" was used for immunohistochemical detection of NF-κB p65 expression in liver of all groups. Paraffin sections were incubated with monoclonal antibody of NF-κB p65 (Dako Corp, Carpenteria, CA) at dilution of 1:200 as well as with the reagents endorsed for "avidin-biotin-peroxidase technique (Vactastain ABC peroxidase kit, Vector Laboratories)". Chromagen "3,3 -diaminobenzidine tetrahydrochloride (DAB, Sigma Chemical Co.)" was used to visualize the marker expression. "Image analysis software Image J, 1.46a, NIH, USA" was used for quantitative image analysis of the optical density of the positive brown color in 5 microscopic fields

2.13- Statistical analysis

The variability of results was expressed as means ± standard error of means. Data were evaluated by one-way analysis of variance (ANOVA) followed by Tukey-Kramer multiple comparisons. The level of significance was accepted at $P < 0.05$.

3- Results

3.1- ZnO/KCl nanocomposite

Fig. 1-a illustrates the XRD patterns of the nanocomposite. The diffraction peaks at 31.83°, 34.47°, 36.35°, 47.61° and 56.64° are indexed to (100), (002), (101), (102) and (110), respectively for standard hexagonal wurtzite structure of ZnO with space group P 63 m c. Peaks at 28.49°, 40.64°, 50.31° and 58.71° are indexed to (200), (220) (222) and (400), respectively for cubic structure of KCl with space group F m -3 m. The crystallographic parameters were computed from the nanocomposite XRD. In case of ZnO-NPs, the values of unit cell parameters a = b and c and interplanar spacing d were calculated from hexagonal wurtzite structure. This equation may be simplified by using planes (100, 002, 101). The calculated cell parameters are a = b = 0.3244 nm, c = 0.5199 nm, interplanar spacing are

d_{100} = 0.2809 nm, d_{001} = 0.2600 nm and d_{101} = 0.2469 nm, axial ratio (a.r.) = 1.6030, unit cell volume (V) = 0.0474 nm^3, oxygen-position parameter (u) = 0.3797 and zinc–oxygen bond length (L) = 0.1974 nm. The calculated cell parameters of KCl are a = b = c = 6.2607. The prime values of cell parameters, atom coordinates, and space group have been taken from equivalent reference patterns, Table 1. Refined structure parameters are listed in Table 1. Structural parameters of ZnO and KCl are listed in Table 2. At the end of the refinement, the obtained results were chi^2 = 1.0 and average Bragg R-factor = 0.05. Vista software was used to calculate the bond length and bond angle from the refined cif files of the nanocomposite, Fig. 1-c, -d, Table 3. The histograms of particles diameters distributions are indicated in Fig. 2-e, -f. The average particle diameters are about 34.51 nm (length). The XPS spectrum of ZnO deconvoluted into two valence states peaked at Zn-$2p_{3/2}$ = 1021.16 eV and Zn-$2p_{1/2}$ = 1044.12 eV binding energies. The XPS spectrum of O-1s showed two peaked at 531.29 eV and 529.56 eV while that of C-1s showed multiple peaks at 284.59, 284.96, 286.27, 288.37 and 289.44.

Table 1 Atomic and structural parameters.

	x	**y**	**z**	**Occ.**	**B**	**Site**	**Lattice parameter**	**Cell Volume (nm3)**
Zn	0.33300 (0.33300)	0.66700 (0.66700)	0.49700 (0.50000)	1.012 (1.000)	0.784 (0.491)	6c (6c)	a = b = 0.3251 (0.3249) nm c = 0.5210 (0.5206) nm α = β = 90° γ = 120°	0.0476 (0.0476)
O	0.66700 (0.66700)	0.33300 (0.33300)	0.37500 (0.37900)	1.302 (1.000)	1.270 (0.459)	6c (6c)		
K	0.00000 (0.00000)	0.00000 (0.00000)	0.00000 (0.00000)	0.998 (1.000)	1.389 (1.000)	4a (4a)	A = b = c = 0.6292 (0.6288) nm α = β = γ = 90°	0.2492 (0.2486)
Cl	0.50000 (0.50000)	0.50000 (0.50000)	0.50000 (0.50000)	1.046 (1.000)	0.175 (1.000)	4b (4b)		

* Refined parameters data (reference code), 96-230-0451 for ZnO and 96-900-3113 for KCl

Table 2 Structural parameters of the ZnO/KCl nanocomposite.

	2θ	FWHM	Crystal size	Microstrain **ε × 10^{-3}**	Specific surface area **S (m^2 g^{-1})**	Lorentz factor **L_f**	Thomson polarization parameter **I_P**	Lorentz polarization parameter **L_P**
ZnO	36.35	0.2755	30.0121	3.6616	35.1909	2.7045	0.8243	17.8352
KCl	28.49	0.1600	50.6564	2.7499	59.4604	4.2598	0.8862	30.2015

Table 3 The calculated bond length and bond angle from the refined cif file of booth phases and the cif files of their reference cards

phase	Bond length (Å)*		Bond angle (deg.)*	
ZnO	O(1)-Zn)	1.96919 (1.97296)	O(1)-Zn- O(1)	108.6968 (108.5516)
			O(1)-Zn- O(2)	108.7230 (108.5775)
	O(2)-Zn	1.97998 (1.97714)	Zn-O(2)- Zn	108.7230 (108.5775)
			O(1)-O(1)- Zn	35.5263 (35.6529)
KCl	Cl(1)-K(1)	3.14620 (3.14395)	Cl(1)-K(1)- Cl(2)	90.0000 (90.0000)
	Cl(2)-K(1)	3.14620 (3.14395)	K(1)- Cl(2)- K(3)	90.0000 (90.0000)

*calculated from refined cif file (calculated from original cif files)

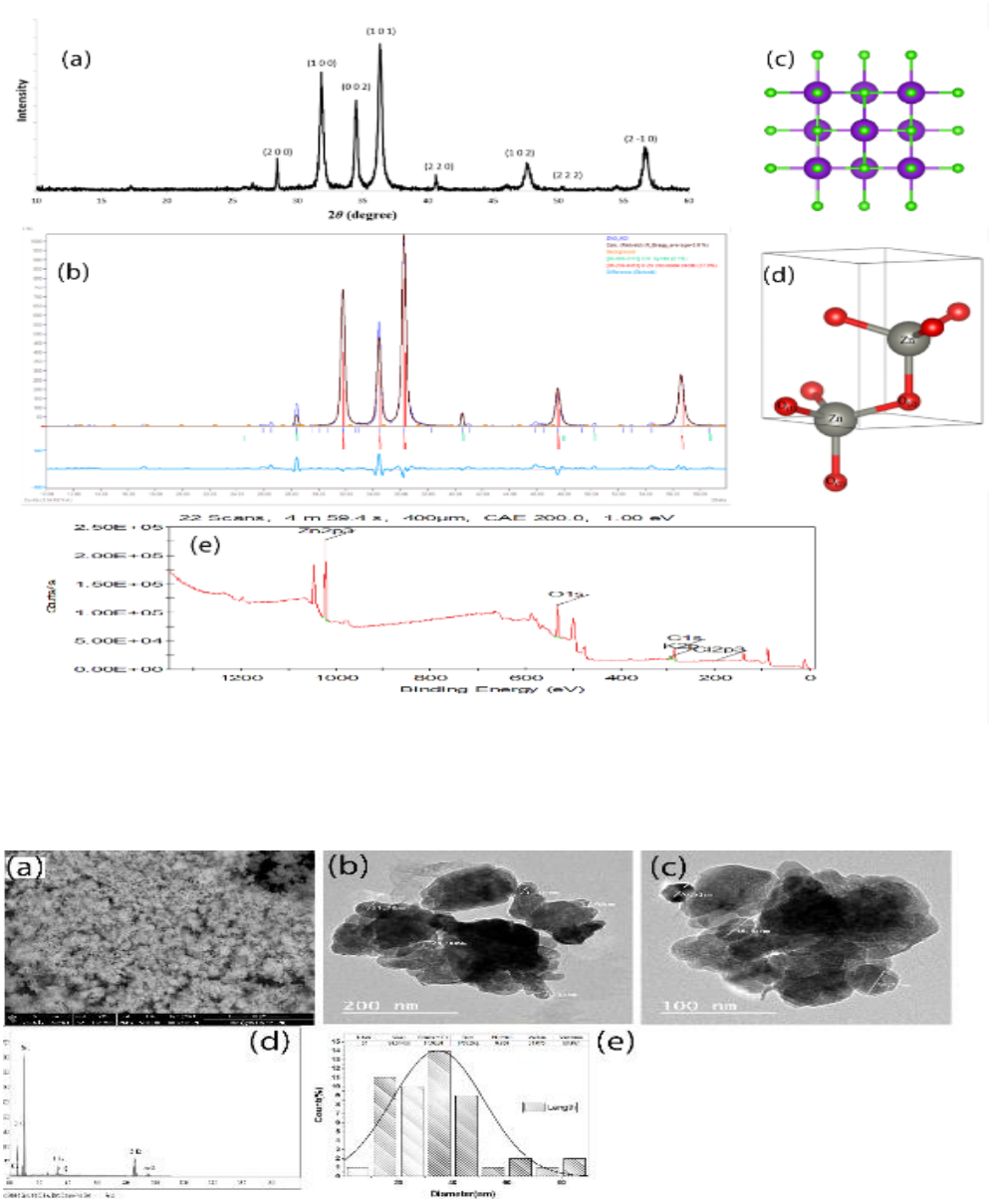

Fig. 2. a) SEM, b-c) HRTEM, d) EDX of the sample, Particle diameters distributions: e) length.formation of c) KCl and d) ZnO, e) XPS survey of ZnO/KCl. nanocomposite.

3.2- Anthropometric measures

The results are represented in fig. 3; indicated a substantial reduction in waist circumference and BMI of obese rats treated with 5 or 10 mg/Kg ZnO-NPs compared to the obese group in all time intervals of the experiment. BMI value in obese rats given 10 mg/Kg ZnO-NPs was significantly less than that of 5 mg/Kg after 6 weeks of treatment. Nevertheless, there has been no substantial change observed in other time intervals. The body gain percentages at six-week post-treatment relative to initial values of control, obese and ZnO-NPs (5 or 10 mg/Kg) were 84%, 191%, 150%, and 140%, respectively.

3.3- Plasma adipocyte hormones

The obese rats exhibited a momentous reduction in adiponectin level and a substantial upsurge in leptin level (Fig. 4). The treatment of obese rats with ZnO-NPs (5 or 10 mg/Kg) modulated these effects.

3.4- Insulin resistance parameters

The treatment of obese rats with ZnO-NPs at dose level of 5 or 10 mg/Kg alleviated the increased plasma insulin or glucose concentration and insulin resistance index (Fig. 4) significantly. Insulin level of high dose of ZnO-NPs is significantly lower than that of low dose, while there is no significant difference between doses of ZnO-NPs on glucose level or IR.

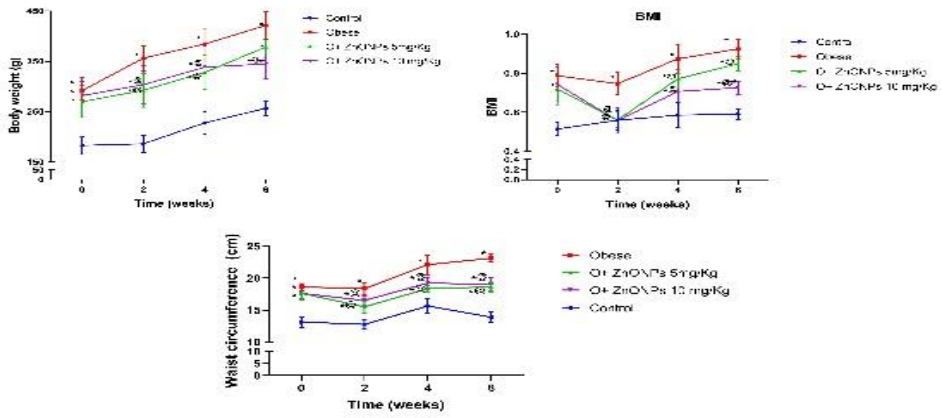

Fig. 3. Effect of ZnO-NPs on anthropometric measures of obese rats. Each value represents the mean of 8 animals ±SE. Statistical analysis was performed using one-way ANOVA followed by Tukey-Kramer multiple comparisons test. (* vs control group, @ vs obese group and # vs ZnO-NPs 5mg/kg) at p<0.05. O: Obese.

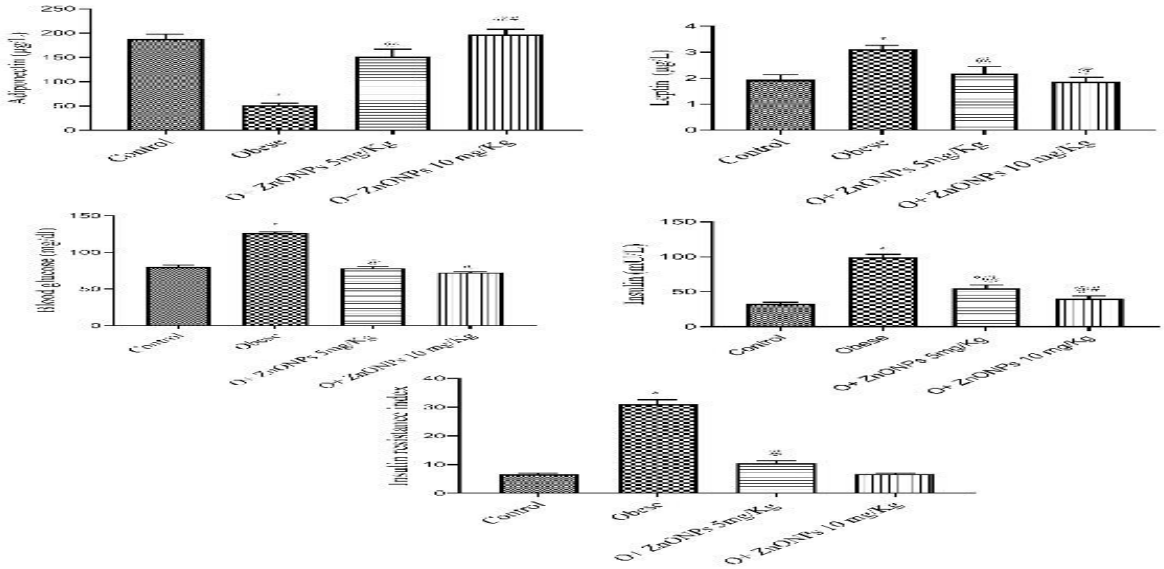

Fig. 4. Effect of ZnO-NPs on plasma adipocyte hormones and insulin resistance in obese rats. Each bar represents the mean of 8 animals ± SE. Statistical analysis was performed using one-way ANOVA followed by Tukey-Kramer multiple comparisons test. (* vs control group, @ vs obese group and # vs O+ ZnO-NP 5mg/kg group) at p<0.05. O: Obese; ZnONP: Zinc oxide nanoparticle.Fig. 1. a) XRD patterns of KCl/ZnO

3.5- Plasma lipid profile

The administration of ZnO-NPs (5 or 10 mg/Kg) to obese rats significantly reduced the elevation of cholesterol, triglycerides and LDL concentrations (Table 4). Also, ZnO-NPs (5 or 10 mg/Kg) given to obese rats preserved HDL levels. The results of high dose of ZnO-NPs were more pronounced than that of low dose.

3.6- Liver function tests

The remediation with low or high doses of ZnO-NPs significantly reduced obesity motivated a significant increase in AST, ALT and GGT levels (Table 5).

Table 4 Effect of ZnO-NPs on plasma lipid profile

Groups	Total cholesterol	Triglycerides	HDL	LDL
Control	90.63±2.76	66.88±1.66	37.57±2.28	21.88±1.27
Obese	197.60±4.97*	231.50±13.63*	7.00±0.46*	87.38±1.90*

O+ZnO-NPs 5mg/kg	131.50±2.77$^{*@}$	200.50±14.47*	28.13±2.35$^{*@}$	43.63±2.21$^{*@}$
O+ZnO-NPs 10mg/kg	87.13±6.58$^{@\#}$	168.60±12.86*@	40.00±2.41$^{@\#}$	25.25±0.88$^{@\#}$

[a] Each value represents the mean of 8 animals ± SE. Statistical analysis was performed using one-way ANOVA followed by Tukey-Kramer multiple comparisons test. (* vs control group, @ vs obese group and # vs ZnO-NPs 5mg/kg) at p<0.05. O: Obese..

Table 5 Effect of ZnO-NPs on Liver function of obese rats

Groups	ALT (U/l)	AST (U/L	GGT (U/L)
Control	29.13±1.46	54.13±2.53	2.53±0.58
Obese	35.88±0.93*	112.90±2.77*	2.77±1.52*
O+ZnO-NPs 5mg/Kg	34.75±1.28*	102.30±4.58*	4.58±0.44$^{@}$
O+ZnO-NPs 10mg/Kg	36.25±1.41*	88.63±6.61$^{*@}$	6.61±0.30$^{@}$

[a] Each value represents the mean of 8 animals ± SE. Statistical analysis was performed using one-way ANOVA followed by Tukey-Kramer multiple comparisons test. (* vs control group, @ vs obese group and # vs ZnO-NPs 5mg/kg) at p<0.05. O: Obese.

3.7- Hepatic oxidative stress and energy parameters

As presented in table 6, the obese rats manifested a significant elevation in the concentration of hepatic MDA, NO, GSSG, 8OHdG, and AMP, on the other hand, hepatic content of GSH, carnitine, and ATP decreased significantly. Injection of obese rats with ZnO-NPs modified the previous parameters. The effect of high dose of ZnO-NPs on GSH, carnitine and ATP is significantly more noticeable than low dose.

3.8- Plasma inflammatory markers

The obese rats administered (IP) ZnO-NPs had markedly lower IL6, TNF-α, and CRP levels than obese rats (Fig. 5). On the other hand, ZnO-NPs injected into obese rats inhibited noticeably the decrease of IL2 level. There is no significant difference between low and high doses of ZnO-NPs in inflammatory markers except CRP that appear significantly low in high dose as compared to low dose. The correlation results (Fig.s 6,7) revealed that there was a positive correlation between BMI and insulin, CRP, TNF-α, IL6, or IR. On the other hand, a negative correlation of BMI with both adiponectin and IL2 was recorded.

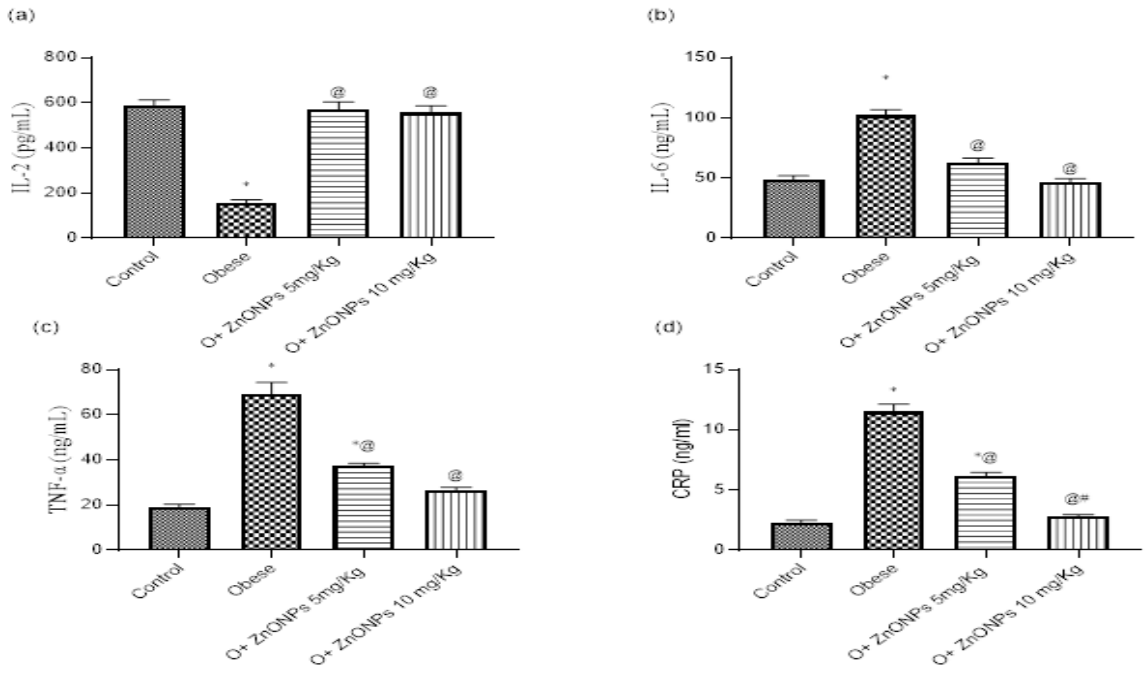

Fig. 5. Effect of ZnO-NPs on plasma inflammatory markers in obese rats. Each bar represents the mean of 8 animals ± SE. Statistical analysis was performed using one-way ANOVA followed by Tukey-Kramer multiple comparisons test. (* vs control group, @ vs obese group and # vs O+ ZnO-NP 5mg/kg group) at p<0.05. O: Obese; ZnONP: Zinc oxide nanoparticleObese; ZnONP: Zinc oxide nanoparticle.

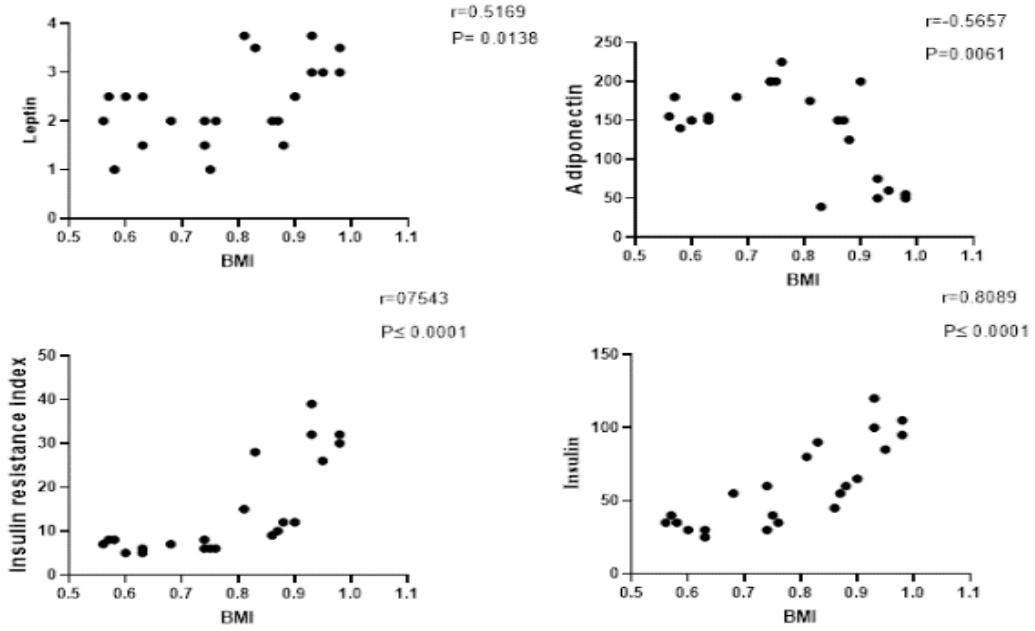

Fig. 6. Correlation of BMI with plasma adipocyte hormones or insulin.

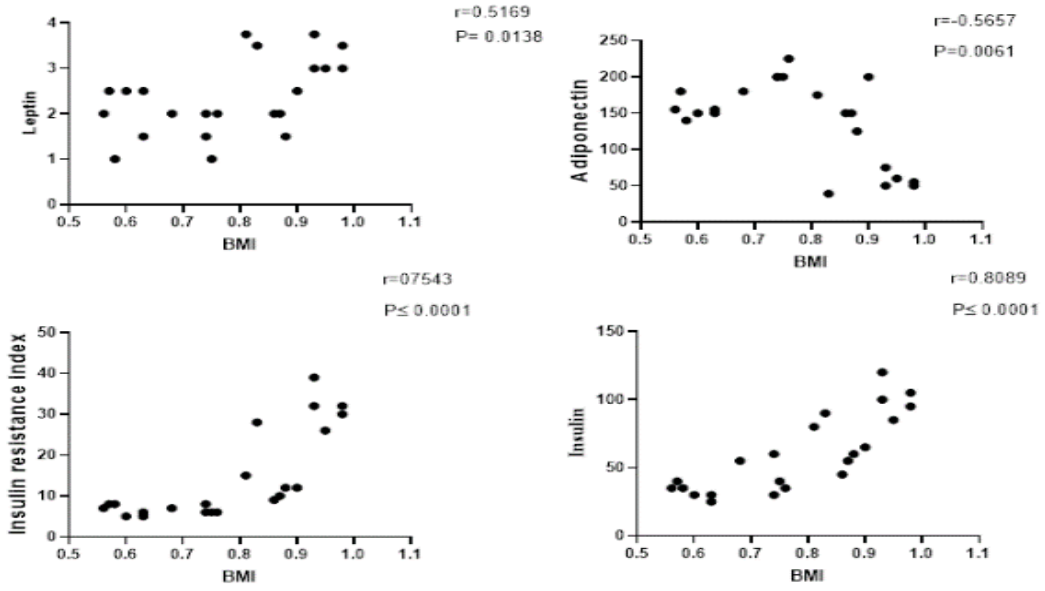

Fig. 7. Correlation of BMI with plasma inflammatory markers.

3.9- Histopathological and immunohistochemical examinations

Examination of liver sections of normal control rats revealed normal histological structure without any obvious changes (Fig. 8 a). While, liver examination of obese rats indicated diffuse hepatic steatosis (Fig. 8 b) predominantly of macro-vesicular type at which the hepatic cells showed marked swelling with presence of one or more large fat vacuoles that pushing the nucleus to one side presenting the shape of signet ring (Fig. 8c). Micro-vesicular steatosis was also notice in a scattered manner. Some hepatocytes appeared ruptured with the release of their fat

contents (ballooning); others, appeared necrotic or apoptotic or appeared bi-nucleated with activated Kupffer cells. Examination of liver sections of the treated groups revealed a dose-related improvement in the hepatic parenchyma cells, on administration of ZnO-NPs at low dose, the hepatic cells showed moderate degree of vacuolar degeneration (Fig. 8d) with scattered necrotic cells as well as few apoptotic cells. While the treatment with ZnO-NPs at the high dose revealed marked retraction of the hepatic steatosis with the scattered appearance of hepatocellular vacuolar degeneration and necrosis (Fig. 8e).

In obese rats, the severity of macro-vesicular steatosis ranged from mild (involvement of one to two third of hepatocytes) to serious (involvement of over than two-thirds of hepatocytes). While in ZnO-NPs treated groups, the criteria of hepatic steatosis were significantly decreased as presented in Fig. 8f. Neither inflammatory foci nor fibrosis was observed in any of the examined groups.

The content of "NFκB-p65" within the hepatocytes of various groups is presented in Fig. 9, which showed marked intense diffuse immune-expression of "NFκB-p65" in the obese group, compared to the control and the treated groups. The latter groups (ZnO-NPs administrated rats) showed a dose-related significant decreased contents of "NF-κB-p65" in hepatocytes as noted by image processing software.

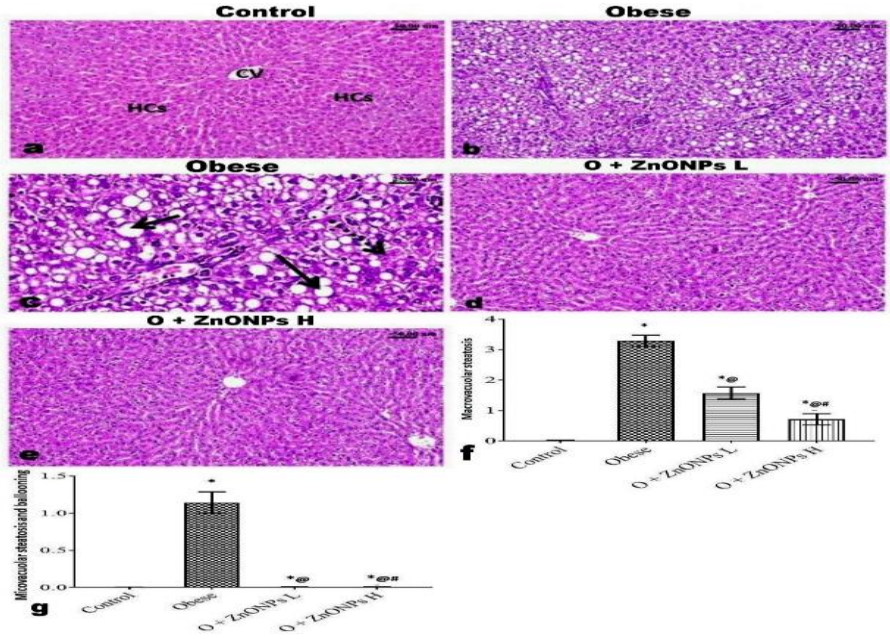

Fig. 8. Photomicrographs of liver sections stained with H&E; (a) Control rat showing normal histologica structure of central vein (CV) and hepatic cells (HCs), (b and c) Obese rat showing diffuse hepatic steatosis particularly of macrovesicular type (b), swollen hepatocytes with presence of one or more large fat vacuoles which pushed the nucleus to one side (arrow), few necrotic cells (dashed arrow) and few ballooned cells (short arrow) (c). (d) ZnO-NPs (low dose) treated rat showing moderate degree of hepatocellular vacuolar degeneration. (e) ZnO-NPs (high dose) treated rat showing scattered hepatocellular vacuolar degeneration and necrosis. (f and g) Numerical scoring of hepatic steatosis in various experimental groups. Each bar represents the mean of 7-11 animals ± SE. Statistical analysis was performed using Kruskal-Wallis test followed by Tukey-Kramer multiple comparisons test. (* vs control group, @ vs obese group and # vs Nano Zn Low group) at $p<0.05$.

4- Discussion

The well-defined sharp peaks in Fig. 1-a indicate that the nanoparticles are well crystallized. The resulted XRD pattern of ZnO and KCl was matched by XRD reference codes 96-230-0451 and 96-900-3113, respectively. The lower intensity of KCl peaks is due to its presence in a lesser amount. These codes were the starting models for the refinement. Debye-Scherrer Method was used in the determination of crystallite sizes. The FWHM (full-width half maximum) of the diffracted peaks were used to calculate the crystallite sizes. FWHM at a lower angle is more meaningful for crystallite size calculation; therefore, the crystallite size of the ZnO was calculated using the high-intensity peak (101) at 2θ value 36.35° and peak (200) at 2θ value 28.49° were used for KCl. Fig. 1-b, -d show

the refinement plots and crystal formation of the sample**, respectively.**

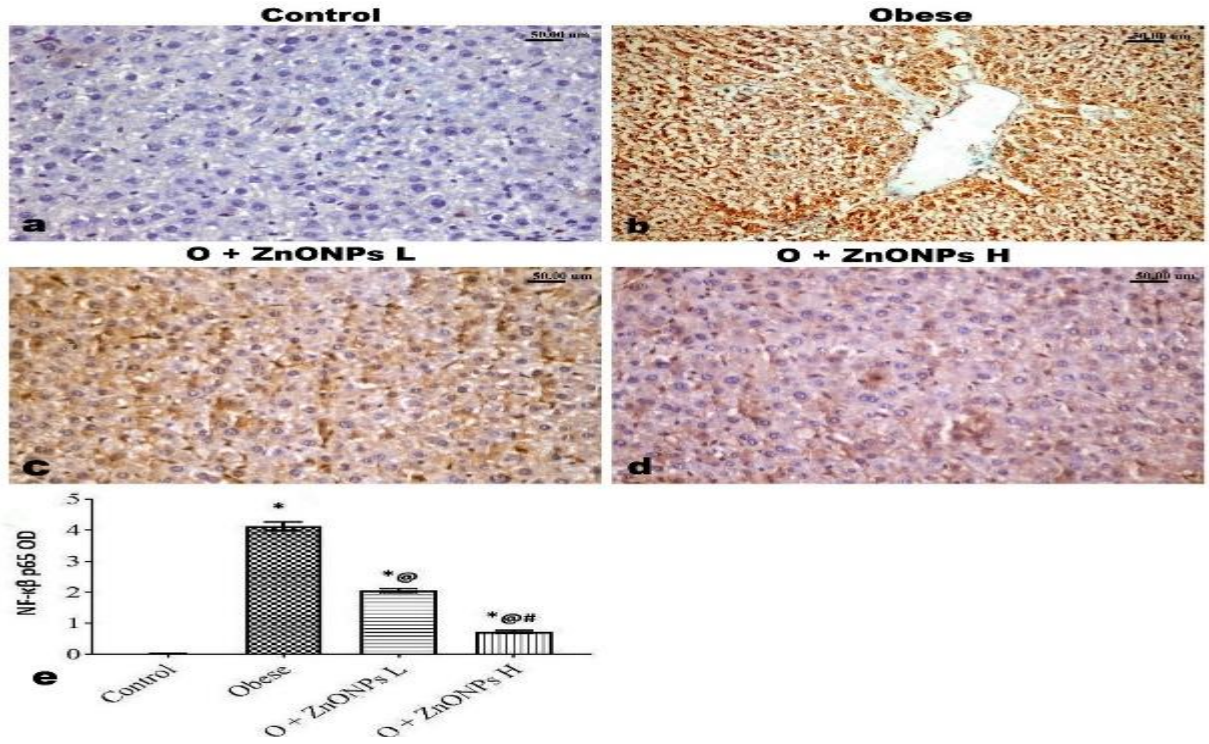

Fig. 9. Photomicrographs of NF-κβ p65-immune-stained liver sections; (a) Negative expression in control group, (b) An intense diffuse expression in obese group, (c and d) Significant dose related decreased expression in ZnO-NPs treated groups, (e) Image analysis of the optical density of the positive brown color. Values are expressed as mean ± SE. Data were analyzed by using one-way ANOVA followed by Tukey post-hoc test.

The Rietveld refinement has been executed via Matche by peak search and fit and then by importing the cif files with the code id 2300450 (ZnO) and 9003112 (KCl) downloaded from COD (Crystallography Open Database). The refinement of profile shape was inspected by pseudo-Voigt function [25]. The Rietveld analysis confirmed hexagonal structure with space group P 63 m c (186) and cubic with space group F m -3 m (225) for ZnO and KCl, respectively. The refined cell parameters were in good agreement with the calculated values. The calculated bond lengths and bond angles after the refinement came with agreement with the starting models Fig. 1-c, -d, Table 3. SEM micrograph was used to examine the sample morphology, Fig. 2-a. The microstructure of the sample has a skeletal form resulting from the process of coagulation. The TEM images (Fig. 2-b, -c) reveal agglomerates of nanoparticles. The EDX spectrum presented in Fig. 2-d, show that only Zn, O and K elements are detected which demonstrated the high purity of the sample. The XPS spectra of the nanocomposite reveal the presence of Cl-2p, K-2p, O-1s and Zn-2p which confirm the presence of ZnO and KCl in the sample. The energy separation between valence states peaked of Zn (Zn-$2p_{3/2}$ and Zn-$2p_{1/2}$) was found to be 22.96 eV with Zn-$2p_{3/2}$ attributed to Zn^{2+} ions bounded in the hexagonal wurtzite structure [26]. The O-1s peak found at 529.56 eV can be assigned to carbonyl or hydroxide group while that at 531.29 eV may be due to the existence of O^2 ions in the ZnO lattice or the presence of chemisorbed oxygen [27]. The C-1s XPS spectrum show characteristic peaks located around 284-288 eV which can be attributed to CO/CO_2, at 289.44 eV assigned to carboxylate carbon [28]. The Cl-2p XPS spectrum shows only one peak at 198.79 eV which can be attributed to the presence of KCl which is further proved by the peak at 292.85 eV in the K-2p XPS spectrum that was also assigned to K-$2p_{3/2}$ in KCl. The later spectrum showed anther peaks at 295.61 eV assigned to K-$2p_{1/2}$ with an energy separation of 2.76.

Zinc has pivotal roles in energy production, appetite goodness and adipokine control (Risk factors related to obesity). It also affects the leptin, insulin and adiponectin hormones, which regulate adiposity and fat mass [29]. In our research, the treatment of obese rats with ZnO-NPs significantly lowered BMI, waist circumference and, body weight gain. The high BMI is connected to the development of obesity since it is parallel to the increase in body fat regarding with

morbidity [30]. The improvement of anthropometric measurements or body weight gain by ZnO-NPs may be attributed to a significant decrease in leptin level or a restoration of adiponectin concentration. It was concluded that obese humans are characterized by high leptin level and leptin resistance [31]. Leptin decreases food intake and increases energy consumption by acting on hypothalamic factors [32]. The treatment of mice fed a high fat/sucrose diet with adiponectin resulted in weight reduction and an increased fatty acid oxidation by muscle [33]. It was reported that body weight control needs decreasing energy intake, and increasing energy-wasting [34].

A significant positive correlation has been recorded between BMI and oxidative stress biomarkers. It appears that ZnO-NPs control BMI of obese rats via reduction of oxidative stress biomarkers, malondialdehyde, GSSG, NO and 8OHdG levels. Moreover, ZnO-NPs injected to obese rats enhanced hepatic GSH and carnitine levels with antioxidant activities [35,36]. ZnO-NPs displayed antioxidant and anti-inflammatory properties [37]. The possible contributors to oxidative stress in obesity include hyperglycemia, elevated lipid levels, chronic inflammation, hyperleptinemia [31,38,39]. It is probably that ZnO-NPs decreases oxidative stress in obese rat directly via their antioxidant properties or indirectly through controlling hyperglycemia, dyslipidemia, hyperleptinemia and inflammation.

The present study demonstrated a significant increase in inflammatory markers, TNF-α, IL6, CRP, and NF-$_k$B due to obesity, while ZnO-NPs treatment lowered these markers. Activation of NF-$_k$B stimulates proinflammatory cytokines production and oxidative stress [40]. The effect of ZnO-NPs on inflammatory markers can be attributed to its effect on leptin level that encourages production of inflammatory cytokines [41]. TNFα is a proinflammatory cytokine suggests a link between obesity, inflammation and T2DM [42]. TNF-α contributes in insulin insensitivity by inhibiting insulin-stimulated tyrosine phosphorylation of the insulin receptor, therefore increasing insulin insensitivity [42]. The blockade of TNF-α signaling might be useful for T2DM and insulin insensitivity [43]. Inflammatory cytokines are linked metabolic and liver disorders, and hence causes insulin resistance and hepatic fat accumulation [44]. Zinc plays an intrinsic role in the prohibition of metabolic syndrome, including insulin resistance, dyslipidemia, and hyperglycemia, through the restraint of proinflammatory cytokine expression, which lowers ROS production, protecting against oxidative stress damage [45].

Obesity is a principal causative factor in the development of metabolic syndrome. Insulin resistance, poor glucose metabolism, and, finally, the development of Type 2 Diabetes Mellitus are all linked to obesity, oxidative stress and fatty liver [46,47]. ZnO-NPs can serve as a new therapeutic agent to preserve the physiological homeostasis during obesity and its associated metabolic abnormalities [7]. Various molecular mechanisms are engaged in the regulation of blood glucose levels following Zinc feeding. Zinc modulated peripheral insulin sensitivity via regulation of protein tyrosine phosphatase, an initiator of the phosphorylation state of the insulin receptor [48]. It appears that ZnO-NPs decreased blood glucose of obese rats via preserving IL2 level, since the exogenous IL-2 treatment can protect mice from diabetes development [49]. Here, ZnO-NPs showed therapeutic effects toward insulin resistance, dyslipidemia and fatty liver observed in obese rats probably via its enhancement effect on adiponectin activity or lowering oxidative stress. Some studies proved that adiponectin minimized obesity associated metabolic dysfunction. Adiponectin has been demonstrated to improve insulin activity and decrease hyperglycemia in diabetic rats [50]. Moreover, adiponectin increases fatty acid oxidation in muscle and reduces free fatty acids and triglycerides [33]. Adiponectin displayed hepatoprotective effect, as it improved the viability of hepatic cells and insulin sensitivity or lessened liver inflammation and fibrosis. Low blood adiponectin level was observed in patients with non-alcoholic steatohepatitis [51]. The observed decrease of fatty liver and insulin resistance in obese rats given ZnO-NPs may be due to their controlling adipokines and cytokines. It was reported that the imbalance of adipokines/cytokines led to generation of insulin resistance, fatty liver and steatosis [52]. It is found that TNF-α or adiponectin has essential role in regulating lipid and glucose metabolism and controlling inflammation in insulin-sensitive tissues. High TNF-α and low adiponectin are linked to NAFLD [53]. Moreover, ZnO-NPs may improve insulin resistance in obese rats by inhibition of NF-κB activation [54] or by decreasing CRP level since high level of CRP is linked with Insulin resistance and hyperinsulinemia [55]. The decrease of fatty liver by ZnO-NPs can be attributed to a reduction of insulin resistance that is considered an initiator factor for steatosis [56]. It was concluded that zinc stimulates lipophagy via peroxisome proliferator–activated receptor alpha pathway and reduces hepatic lipid deposition leading to improved fatty liver [5]. Zinc supplementation to obese patients significantly reduced ALT, GGT and steatosis [57]. Here, ZnO-NPs injected to obese rats lowered hepatic pathological changes. It was suggested that ZnO-NPs protect liver damage induced by thioacetamide through lowering inflammatory markers and lipid peroxidation or improving antioxidant status [6].

Also, ZnO-NPs prohibited the decrease in hepatic ATP observed in obese rats that may refer to its antioxidant property since reactive oxygen species lead to a disturbance in mitochondrial function [58]. Insulin resistance and T2DM are linked to a reduction in the activity of mitochondria, which causes the formation of ectopic fat in muscle. Severe insulin resistance is linked to considerably increased levels of triglycerides in both muscle and liver in the patient with type 2 diabetes and insulin resistance. These alterations were followed by declines in mitochondria-induced oxidation and ATP production, both of which indicate a loss in mitochondria function [59].

Table 6 Effect of ZnO-NPs on hepatic oxidative stress and energy parameters of obese rats

Parameters	Control	Obese	O+ZnO-NPs 5mg/Kg	O+ZnO-NPs 10mg/Kg
MDA (nmol/g tissue)	13.84±0.57	19.22±0.79*	16.87±0.67*	15.98±0.59@
GSH (µmol/g tissue)	3.50±0.07	1.40±0.02*	1.87±0.05*@	2.52±0.056*@#
GSSG (µmol/g tissue)	0.33±0.01	0.47±0.01*	0.39±0.01*@	0.39±0.01*@
NO (µmol/g tissue)	14.20±0.77	18.66±0.44*	17.74±0.56@	17.09±0.47@
8OHdG (pg/g tissue)	137.20±3.17	202.40±5.86*	189.5±7.06*	171.0±2.79*@
Car (nmol/g tissue)	46.02±2.09	4.57±0.19*	13.01±0.81*@	23.58±1.42*@#
ATP (µg/g tissue)	47.76±1.83	5.20±0.32*	15.25±1.82*@	23.66±1.15*@#
AMP (µg/g tissue)	10.76±0.47	15.37±0.68*	14.26±0.47*	12.84±0.49@

[a] Each value represents the mean of 8 animals ± SE. Statistical analysis was performed using one-way ANOVA followed by Tukey-Kramer multiple comparisons test. (* vs control group, @ vs obese group and # vs ZnO-NPs 5mg/kg) at $p<0.05$, O: Obese, Car: Carnitine.

5- Conclusions

the treatment of obese rats with ZnO-NPs showed efficient therapeutic effect in alleviation symptoms of obesity and its complications as insulin resistance, type 2 diabetes and fatty liver probably by decreasing oxidative stress, lipids and inflammatory markers or improving antioxidant defense system.

6- Conflicts of interest

There are no conflicts to declare.

7- Formatting of funding sources

This work is financially supported by National Research Centre, Cairo, Egypt (Project No 12060157)

8- References

[1] Salata, O. Applications of nanoparticles in biology and medicine. *journal nanobiotechnology*, **2**, 3-8 (2004).

[2] Zhang, Y.; Nayak, T. R.; Hong, H.; Cai, W. Biomedical Applications of Zinc Oxide Nanomaterials. *Current Molecular Medicine*, **13** (10), 1633–1645 (2013).

[3] Jiang, J.; Pi, J.; Cai, J. The Advancing of Zinc Oxide Nanoparticles for Biomedical Applications. *Bioinorganic Chemistry and Applications*, ***2018***, 1062562 (2018).

[4] El-Tabl, A. S.; Shakdofa, M. M. E.; El-Seidy, A. M. A.; Al-Hakimi, A. N. Synthesis, Characterization and Antifungal Activity of Metal Complexes of 2-(5-((2-Chlorophenyl)Diazenyl)-2-Hydroxybenzylidene) Hydrazinecarbothioamide. *Phosphorus, Sulfur, and Silicon and the Related Elements*, **187** (11), 1312–1323 (2012).

[5] Wei, C.-C.; Luo, Z.; Hogstrand, C.; Xu, Y.-H.; Wu, L.-X.; Chen, G.-H.; Pan, Y.-X.; Song, Y.-F. Zinc Reduces Hepatic Lipid Deposition and Activates Lipophagy via Zn(2+)/MTF-1/PPARα and Ca(2+)/CaMKKβ/AMPK Pathways. FASEB Journal, **32**(12) 6666-6680 (2018).

[6] Bashandy, S. A. E.; Alaamer, A.; Moussa, S. A. A.; Omara, E. A. Role of Zinc Oxide Nanoparticles in Alleviating Hepatic Fibrosis and Nephrotoxicity Induced by Thioacetamide in Rats. *Canadian Journal of Physiology and Pharmacology*, **96** (4), 337–344 (2018).

[7] Dogra, S.; Kar, A. K.; Girdhar, K.; Daniel, P. V.; Chatterjee, S.; Choubey, A.; Ghosh, S.; Patnaik, S.; Ghosh, D.; Mondal, P. Zinc Oxide Nanoparticles Attenuate Hepatic Steatosis Development in High-Fat-Diet Fed Mice through Activated AMPK Signaling Axis. *Nanomedicine Nanotechnol. Biol. Med.* 2019, *17*, 210–222. https://doi.org/10.1016/j.nano.2019.01.013.

[8] Nagajyothi, P. C.; Cha, S. J.; Yang, I. J.; Sreekanth, T. V. M.; Kim, K. J.; Shin, H. M. Antioxidant and Anti-Inflammatory Activities of

Zinc Oxide Nanoparticles Synthesized Using Polygala Tenuifolia Root Extract. *Journal of Photochemistry and Photobiology B: Biology*, **146**, 10–17 (2015).

[9] Kim, J.; Ahn, J. Effect of Zinc Supplementation on Inflammatory Markers and Adipokines in Young Obese Women. *Environmental Biology of Fishes*, **157** (2), 101–106 (2014).

[10] Payahoo, L.; Ostadrahimi, A.; Mobasseri, M.; Khaje Bishak, Y.; Farrin, N.; Asghari Jafarabadi, M.; Mahluji, S. Effects of Zinc Supplementation on the Anthropometric Measurements, Lipid Profiles and Fasting Blood Glucose in the Healthy Obese Adults. *Advanced Functional Materials*, *3* (1), 161–165 (2013).

[11] Marreiro, D. do N.; Geloneze, B.; Tambascia, M. A.; Lerário, A. C.; Halpern, A.; Cozzolino, S. M. F. Effect of Zinc Supplementation on Serum Leptin Levels and Insulin Resistance of Obese Women. *Biological Trace Element Research*, **112** (2), 109–118 (2006).

[12] Lim, J. S.; Mietus-Snyder, M.; Valente, A.; Schwarz, J.-M.; Lustig, R. H. The Role of Fructose in the Pathogenesis of NAFLD and the Metabolic Syndrome. *Nature Reviews Gastroenterology & Hepatology*, **7** (5), 251–264 (2010).

[13] Hurt, R. T.; Kulisek, C.; Buchanan, L. A.; McClave, S. A. The Obesity Epidemic: Challenges, Health Initiatives, and Implications for Gastroenterologists. *Journal of Gastroenterology and Hepatology*, **6** (12), 780–792 (2010).

[14] Seidell, J. C.; Halberstadt, J. The Global Burden of Obesity and the Challenges of Prevention. *Annals of Nutrition and Metabolism*, **66** *Suppl 2*, 7–12 (2015).

[15] Calcaterra, V.; Regalbuto, C.; Porri, D.; Pelizzo, G.; Mazzon, E.; Vinci, F.; Zuccotti, G.; Fabiano, V.; Cena, H. Inflammation in Obesity-Related Complications in Children: The Protective Effect of Diet and Its Potential Role as a Therapeutic Agent. *Biomolecules*, **10** (9), 1324 (2020).

[16] Tiniakos DG, Vos MB, Brunt EM. Nonalcoholic fatty liver disease: pathology and pathogenesis. Annual Review of Pathology, **5,** 145-71 (2010).

[17] Brunt, E. M. Pathology of Non-alcoholic Fatty Liver Disease. *Nature Reviews Gastroenterology & Hepatology*, **7** (4), 195–203 (2010).

[18] Zaki, M.; Ezzat, W.; Elhosary, Y.; Saleh, O. Predictors of Non-Alcoholic Fatty Liver Disease in Egyptian Obese Adolescents. *International Journal of Medical, Medicine and Health Sciences*, **8** (9), 685–688 (2014).

[19] Gregor, M. F.; Hotamisligil, G. S. Inflammatory Mechanisms in Obesity. *Annual Review of Immunology*, **29**, 415–445 (2011).

[20] Gurzov, E. N.; Tran, M.; Fernandez-Rojo, M. A.; Merry, T. L.; Zhang, X.; Xu, Y.; Fukushima, A.; Waters, M. J.; Watt, M. J.; Andrikopoulos, S.; Neel, B. G.; Tiganis, T. Hepatic Oxidative Stress Promotes Insulin-STAT-5 Signaling and Obesity by Inactivating Protein Tyrosine Phosphatase N2. *Cell Metabolism*, **20** (1), 85–102 (2014).

[21] Makki, K.; Froguel, P.; Wolowczuk, I. Adipose Tissue in Obesity-Related Inflammation and Insulin Resistance: Cells, Cytokines, and Chemokines. *ISRN Inflammation*, **2013**, 139239 (2013).

[22] Teerlink, T.; Hennekes, M.; Bussemaker, J.; Groeneveld, J. Simultaneous Determination of Creatine Compounds and Adenine Nucleotides in Myocardial Tissue by High-Performance Liquid Chromatography. *Analytical Biochemistry*, **214** (1), 278–283 (1993).

[23] Lodovici, M.; Casalini, C.; Briani, C.; Dolara, P. Oxidative Liver DNA Damage in Rats Treated with Pesticide Mixtures. *Toxicology*, **117** (1), 55–60 (1997).

[24] Brunt, E. M.; Janney, C. G.; Di Bisceglie, A. M.; Neuschwander-Tetri, B. A.; Bacon, B. R. Non-alcoholic Steatohepatitis: A Proposal for Grading and Staging the Histological Lesions. *American Journal of Gastroenterology*, **94** (9), 2467–2474 (1999).

[25] Bagheri, S. Facile Synthesis of Nano-Sized ZnO by Direct Precipitation Method. *Scholars Research Library*, **65**(3), 265-270 (2013).

[26] Antony, A.; Poornesh, P.; Kityk, I. V.; Ozga, K.; Jedryka, J.; Rakus, P.; Wojciehcowski, A. X-Ray Photoelectron Spectroscopy, Raman and Photoluminescence Studies on Formation of Defects in Cu:ZnO Thin Films and Its Role in Nonlinear Optical Features. *Laser Physics*, **28** (9), 095405 (2018).

[27] Khokhra, R.; Bharti, B.; Lee, H.-N.; Kumar, R. Visible and UV Photo-Detection in ZnO Nanostructured Thin Films via Simple Tuning of Solution Method. *Scientific Reports*, **7,** 15032 (2017).

[28] Otgonbayar, Z.; Fatema, K. N.; Yang, S.; Kim, I.-J.; Kim, M.; Shim, S. E.; Oh, W.-C. Temperature Dependence for High Electrical Performance of Mn-Doped High Surface Area Activated Carbon (HSAC) as Additives for Hybrid Capacitor. *Scientific Reports*, **11** (1), 534 (2021).

[29] Hashemipour, M.; Kelishadi, R.; Shapouri, J.; Sarrafzadegan, N.; Amini, M.; Tavakoli, N.; Movahedian-Attar, A.; Mirmoghtadaee, P.; Poursafa, P. Effect of Zinc Supplementation on

Insulin Resistance and Components of the Metabolic Syndrome in Prepubertal Obese Children. *HORMONES*, **8** (4), 279–285 (2009).

[30] Baik, I.; Ascherio, A.; Rimm, E. B.; Giovannucci, E.; Spiegelman, D.; Stampfer, M. J.; Willett, W. C. Adiposity and Mortality in Men. *American Journal of Epidemiology*, **152** (3), 264–271 (2000).

[31] Berger, S.; Polotsky, V. Y. Leptin and Leptin Resistance in the Pathogenesis of Obstructive Sleep Apnea: A Possible Link to Oxidative Stress and Cardiovascular Complications. *Oxidative Medicine and Cellular Longevity*, **2018**, 5137947 (2018).

[32] Ahima, R. S.; Prabakaran, D.; Mantzoros, C.; Qu, D.; Lowell, B.; Maratos-Flier, E.; Flier, J. S. Role of Leptin in the Neuroendocrine Response to Fasting. *Nature*, **382** (6588), 250–252 (1996).

[33] Fruebis, J.; Tsao, T. S.; Javorschi, S.; Ebbets-Reed, D.; Erickson, M. R.; Yen, F. T.; Bihain, B. E.; Lodish, H. F. Proteolytic Cleavage Product of 30-KDa Adipocyte Complement-Related Protein Increases Fatty Acid Oxidation in Muscle and Causes Weight Loss in Mice. *Proceedings of the National Academy of Sciences*, **98** (4), 2005–2010 (2001).

[34] Chong, P.-W.; Beah, Z.-M.; Grube, B.; Riede, L. IQP-GC-101 Reduces Body Weight and Body Fat Mass: A Randomized, Double-Blind, Placebo-Controlled Study. *Phytotherapy Research*, **28** (10), 1520–1526 (2014). https://doi.org/10.1002/ptr.5158.

[35] Kerksick, C.; Willoughby, D. The Antioxidant Role of Glutathione and N-Acetyl-Cysteine Supplements and Exercise-Induced Oxidative Stress. *Journal of the International Society of Sports Nutrition*, **2** (2), 38-44 (2005).

[36] Kujala, T.S.; Loponen, J.M.; Klika, K.D.; Pihlaja, K. Phenolics and betacyanins in red beetroot (Beta vulgaris) root: Distribution and effect of cold storage on the content of total phenolics and three individual compounds. J. Agric. *Food Chemistry*, **48**, 5338–5342 (2000).

[37] Mohapatra, S.; Leelavathi, L.; Rajeshkumar, S.; Sri Sakthi, D.; Jayashri, P. Assessment of Cytotoxicity, Anti-Inflammatory and Antioxidant Activity of Zinc Oxide Nanoparticles Synthesized Using Clove and Cinnamon Formulation--An In-Vitro Study. *Journal of evolution of medical and dental science*, **9**, 1859-1864 (2020).

[38] Li, J.; Shen, X. Oxidative Stress and Adipokine Levels Were Significantly Correlated in Diabetic Patients with Hyperglycemic Crises. *Diabetology & Metabolic Syndrome*, **11** (1), 13 (2019). https://doi.org/10.1186/s13098-019-0410-5.

[39] Matsuda, M.; Shimomura, I. Increased Oxidative Stress in Obesity: Implications for Metabolic Syndrome, Diabetes, Hypertension, Dyslipidemia, Atherosclerosis, and Cancer. *Obesity Research & Clinical Practice*, **7** (5), e330-41 (2013).

[40] Bondia-Pons, I.; Ryan, L.; Martinez, J. A. Oxidative Stress and Inflammation Interactions in Human Obesity. *Journal of Physiology and Biochemistry*, **68** (4), 701–711 (2012).

[41] Parola, M.; Marra, F. Adipokines and Redox Signaling: Impact on Fatty Liver Disease. *Antioxidants & Redox Signaling*, ***15*** (2), 461–483 (2011).

[42] Alzamil, H. Elevated Serum TNF-α Is Related to Obesity in Type 2 Diabetes Mellitus and Is Associated with Glycemic Control and Insulin Resistance. *Journal of Obesity*, **2020**, 5076858 (2020).

[43] Akash, M. S. H.; Rehman, K.; Liaqat, A. Tumor Necrosis Factor-Alpha: Role in Development of Insulin Resistance and Pathogenesis of Type 2 Diabetes Mellitus. *Journal of Cellular Biochemistry*, **119** (1), 105–110 (2018).

[44] Das, S. K.; Balakrishnan, V. Role of Cytokines in the Pathogenesis of Non-Alcoholic Fatty Liver Disease. *Indian Journal of Clinical Biochemistry*, **26** (2), 202–209 (2011).

[45] Olechnowicz, J.; Tinkov, A.; Skalny, A.; Suliburska, J. Zinc Status Is Associated with Inflammation, Oxidative Stress, Lipid, and Glucose Metabolism. *The Journal of Physiological Sciences*, **68** (1), 19–31 (2018).

[46] Aydin, S.; Aksoy, A.; Aydin, S.; Kalayci, M.; Yilmaz, M.; Kuloglu, T.; Citil, C.; Catak, Z. Today's and Yesterday's of Pathophysiology: Biochemistry of Metabolic Syndrome and Animal Models. *Nutrition*, **30** (1), 1–9 (2014).

[47] Hafizi Abu Bakar, M.; Kian Kai, C.; Wan Hassan, W. N.; Sarmidi, M. R.; Yaakob, H.; Zaman Huri, H. Mitochondrial Dysfunction as a Central Event for Mechanisms Underlying Insulin Resistance: The Roles of Long Chain Fatty Acids. *Diabetes/Metabolism Research and Reviews*, **31** (5), 453–475 (2015).

[48] Haase, H.; Maret, W. Protein Tyrosine Phosphatases as Targets of the Combined Insulinomimetic Effects of Zinc and Oxidants. *BioMetals*, **18** (4), 333–338 (2005).

[49] Hulme, M. A.; Wasserfall, C. H.; Atkinson, M. A.; Brusko, T. M. Central Role for Interleukin-2 in Type 1 Diabetes. *Diabetes*, **61** (1), 14–22 (2012).

[50] Berg, A. H.; Combs, T. P.; Du, X.; Brownlee, M.; Scherer, P. E. The Adipocyte-Secreted Protein Acrp30 Enhances Hepatic

Insulin Action. *Nature Medicine*, **7** (8), 947–953 (2001).

[51] Polyzos, S. A.; Kountouras, J.; Zavos, C.; Tsiaousi, E. The Role of Adiponectin in the Pathogenesis and Treatment of Non-Alcoholic Fatty Liver Disease. *Diabetes, Obesity and Metabolism*, **12** (5), 365–383 (2010).

[52] Jarrar, M. H.; Baranova, A.; Collantes, R.; Ranard, B.; Stepanova, M.; Bennett, C.; Fang, Y.; Elariny, H.; Goodman, Z.; Chandhoke, V.; Younossi, Z. M. Adipokines and Cytokines in Non-Alcoholic Fatty Liver Disease. *Alimentary Pharmacology & Therapeutics*, **27** (5), 412–421 (2008).

[53] Hui, J. M.; Hodge, A.; Farrell, G. C.; Kench, J. G.; Kriketos, A.; George, J. Beyond Insulin Resistance in NASH: TNF-Alpha or Adiponectin? *Hepatologists*, **40** (1), 46–54 (2004).

[54] Xie, F.; Zhu, J.; Hou, B.; Wang, Y.; Meng, F.; Ren, Z.; Ren, S. Inhibition of NF-KB Activation Improves Insulin Resistance of L6 Cells. *Endocrine Journal*, **64** (7), 685–693 (2017).

[55] Yang, J. S.; Gerber, J. N.; You, H. J. Association between Fasting Insulin and High-Sensitivity C Reactive Protein in Korean Adults. *British Journal of Sports Medicine*, **3** (1), e000236 (2017).

[56] Than, N. N.; Newsome, P. N. A Concise Review of Non-Alcoholic Fatty Liver Disease. *Atherosclerosis*, **239** (1), 192–202 (2015).

[57] Fathi, M.; Alavinejad, P.; Haidari, Z.; Amani, R. The Effect of Zinc Supplementation on Steatosis Severity and Liver Function Enzymes in Overweight/Obese Patients with Mild to Moderate Non-Alcoholic Fatty Liver Following Calorie-Restricted Diet: A Double-Blind, Randomized Placebo-Controlled Trial. *Biological Trace Element Research*, **197** (2), 394–404 (2020).

[58] Guo, C.; Sun, L.; Chen, X.; Zhang, D. Oxidative Stress, Mitochondrial Damage and Neurodegenerative Diseases. *Neural Regeneration Research*, **8** (21), 2003–2014 (2013).

[59] Petersen, K. F.; Dufour, S.; Shulman, G. I. Decreased Insulin-Stimulated ATP Synthesis and Phosphate Transport in Muscle of Insulin-Resistant Offspring of Type 2 Diabetic Parents. *PLOS Medicine*, **2** (9), e233 (2005).